PREPARATION OF BORIC ACID MODIFIED EXPANDABLE GRAPHITE AND ITS INFLUENCE ON POLYETHYLENE COMBUSTION CHARACTERISTICS

HONGMEI ZHAO[a,b], XIUYAN PANG[a], RUINIAN LIN[a]*

[a]*llege of Chemistry and Environmental Science, Key Laboratory of Analytical Science and Technology of Hebei Province, Hebei University, Baoding 071002, PR China*
[b]*Department of VIP, Affiliated Hospital of Hebei University, Baoding, Hebei 071000, PR China*

ABSTRACT

A boric acid modified expandable graphite (EG_B) was prepared through oxidizing-intercalating reaction of natural graphite, using H_2SO_4 and boric acid (H_3BO_3) as intercalators simultaneously. The dilatability of the intercalated products were characterized with expansion volume and initial expansion temperature. Scanning electron microscope, X-ray diffraction spectroscopy, energy dispersive spectroscopy and Fourier transform infrared spectroscopy were employed to detect its layer structure, main element relative contents and function group. At the same time, its influence on combustion characteristics and thermal stability for linear low density polyethylene (LLDPE) were investigated in limiting oxygen index (LOI) tests, vertical burning tests and thermal gravimetric/differential thermal gravimetric analyses. Comparing with the normal expandable graphite (EG, intercalated by single H_2SO_4), EG_B exhibited high dilatability, thermal stability and flame retardancy for LLDPE. It had been testified by combustion tests that the addition of 30 wt % EG_B to LLDPE improved the limiting oxygen index (LOI) from 17.6% to 30.2%, and the vertical burning level of UL-94 standard reached V-0 level. Whereas, the LOI of the same amount referenced EG was only 25.1%, the UL-94 level only reached V-1. Moreover, the synergistic effect between EG_B and ammonium polyphosphate (II) (APP) improved the LOI of 70LLDPE/10APP/20EG_B composite to 33.0%, and the UL-94 level to V-0. The synergistic efficiency was attributed to the formation of continuous and compact residual char.

Keywords: Modified expandable graphite; boric acid; characteristics; dilatability; flame retardancy; synergistic efficiency.

INTRODUCTION

Natural graphite is a kind of carbon material with layer structure, intercalator such as sulfuric acid can be included between the carbon layers in chemical or electronic chemical oxidation reaction, [1, 2] and then graphite intercalating compound (GIC) named expandable graphite (EG) is obtained. EG is known as a new generation of intumescent flame retardant (IFR) for its good capability of halogen-free, non-dropping and low-smoke. [3, 4] This retardant acts in both the condensed and gas phase through an endothermic reaction: [5, 6] (1) when contacting with flame source, EG will instantly expand and turn into swollen multicellular "graphite worms" covering on the retarded polymer surface, which is in favor of slowing down the heat and mass transfer and interrupting the degradation of polymer matrix. (2) In oxidation reaction with H_2SO_4 at high temperature, it releases gases such as CO_2, H_2O and SO_2, [3, 7-9] which can reduce concentration of combustible gas; thereby char formation has been enhanced. (3) Expansion of EG will consume an enormous amount of heat, which is helpful to decrease the combustion temperature and rate.

Due to its outstanding anti-flame capability, EG has been used in the flame retardance of polymer materials such as polyurethane (PU) or polyurethane coatings, [10, 11] polyolefin blends, [12, 13] acrylonitrile-butadiene-styrene (ABS), [14, 15] ethylene vinyl acetate (EVA). [16, 17] However, there are still some shortcomings when EG is used as a FR. Firstly, due to its limited efficiency, a normal 30 wt% dose is needed to achieve satisfying effect, [18] which often leads to obvious deterioration of the mechanical properties. Moreover, more SO_2 will emit when EG is prepared with only H_2SO_4 as intercalator. [19, 20] So it is very important to enhance efficiency in order to meet environmental protection standard.

Measures have been attempted to improve EG flame retardancy and reduce its dose. Addition of EG together with other synergistic FRs such as phosphonate, [21] polyphosphate, [22] phosphorus, [23] metal hydroxide, [12] layered double hydroxide, [24] silica, [25] had been tested, and results indicated the addition of other synergistic FRs can normally improve flame retardancy and reduce EG dose. Surface treatments had been also reported to improve EG miscibility with polymer matrices. Hao et al prepared an EG modified with silane coupling agent and boric acid, [26] and its application for PU indicated that thermal stability of the modified EG and its flame retardancy for PU composites were all higher than that of normal EG. While, the ground EG treated with phosphoric acid and silane presented an obvious increase of volume expansion ratio, [15] and addition of the treated EG in ABS significantly enhanced the fire performance but decreased the impact strength of ABS. Whereas, the improvement by combined addition or EG modification is usually very limited, especially the simple mix of EG with other retardants. [17] The main reason should be the insufficient mix caused by the inconsistence of particle size, density, polarity and addition dosage between these FRs and matrix.

It is worthy to note that non-carbon substance can easily move into the graphite layers and form GIC with accordant components. [27] Therefore, if a FR is used as assistant intercalator, the combined retardant can be prepared through graphite intercalating reaction, which can not only reduce sulfur content in GIC, but also improve the mix uniformity and then improve EG dilatability and flame retardancy. It was reported the H_2SO_4/APP (APP, ammonium polyphosphate, a assistant intercalating agent) GIC, prepared through two-step method, exhibited a higher expansion volume (EV, 240 mL g^{-1}) than that of the H_2SO_4 intercalated EG (210 mL g^{-1}). [19] An EG, intercalated by H_2SO_4 and Na_2SiO_3 through two-step intercalation reaction, [17] presented an EV of 517 mL g^{-1} and combustion limiting oxygen index (LOI) of 28.7% for EVA. However, the EV of referenced EG, which is intercalated by only H_2SO_4 was merely 433 mL g^{-1}, and the LOI was just 24.4%. At the same time, its relative sulfur content decreased from 1.79% to 1.23%. Especially, the intercalated Na_2SiO_3 in EG is more effectual in improving the flame retardancy than the direct addition of $Na_2SiO_3 \cdot 9H_2O$ with EG.

According to the former researches, B and boric acid (H_3BO_3) have been widely used as oxidation inhibitors to improve the thermal stability of carbon materials. With boron oxide as precursor, [28] the B modified carbon fiber reinforce carbon (CFRC) composite could be prepared with soaking or direct mixing method, and the results showed the incorporation of B in CFRC was beneficial for the improving of crystallinity and oxidation stability. Saidaminova *et al* prepared a H_3BO_3 modified EG through electrochemical oxidation of graphite-H_2SO_4-H_3BO_3 system, [29] and the results showed that the modified EG possessed higher thermal stability by 200 °C than the referenced EG. And then, the oxidized graphite was synthesized with chemical oxidation method in the graphite-H_2SO_4-H_3BO_3-$K_2Cr_2O_7$ system, [30] and the modification raised the oxidation onset temperature by 200-300°C. In fact, H_3BO_3 is not only an oxidation inhibitor, but also a well-known halogen-free, non-toxic and smoke suppressing FR. H_3BO_3 can absorb heat and dehydrate at lower temperature due to its lower melting point. It acts in both the condensed phase and gas phase through an endothermic reaction. The released water vapour can reduce concentration of combustible gas, and furthermore, the residual boric oxide can form a glassy coating on polymer surface, limiting the transfer of heat and mass, as well as oxygen diffusion, and then retarding further combustion. Thereby, H_3BO_3 is a kind of FR with good flame retardancy, and it can be solely added or used together with others to get better efficiency. [31-34]

To get a kind of EG with low the sulfur content, well dilatability and flame retardancy, this research is to prepare H_3BO_3 modified EG (written as EG_B) through flake graphite intercalation reaction with H_2SO_4 as main intercalator and H_3BO_3 as assistant intercalator simultaneously. The preparation method was founded and energy dispersive spectroscopy (EDS) was used to confirm the change of sulfur relative content. Scanning electron microscope, X-ray diffraction spectroscopy (XRD) and Fourier transform infrared spectroscopy (FTIR) were employed to characterize the structure and main functional group. Meanwhile, with linear low density polyethylene (LLDPE) as flame retarded matrix, the flame retardancy of EG_B, referenced EG (intercalated with only H_2SO_4), H_3BO_3 and EG/H_3BO_3 (a mechanical mixture) were all tested. Furthermore, to improve the LOI value, vertical combustion UL-94 level

e-mail: pxy833@163.com

and suppress the existed "popcorn effect" simultaneously, APP was added together in view of the reported synergistic effect between the two retardants. [35, 36] LOI and UL-94 rating tests, thermal gravimetric and differential thermal gravimetric (TG/DTG) analyses were performed to investigate the flame retarded performance and the thermal stability. Electron microscope was applied to observe the residual char morphology.

EXPERIMENTAL

Raw Materials and Sample Preparation: Natural flake graphite (average particle size of 0.30 mm, carbon content of 92%) was provided by Action Carbon CO. LTD, Baoding, China. LLDPE (7042, 0.918 g cm^{-3}, melt index 2.0 g min^{-1}) was purchased from Tianjin, China. APP (II, n>1000) was purchased from Sichuan, China. H_3BO_3 and H_2SO_4 (98%) were all analytical reagents and used as received.

Preparation of EG_B and the referenced EG: Firstly, the reactants were weighed according to a definite mass ratio of graphite C:H_2SO_4(98%):$KMnO_4$:H_3BO_3, and H_2SO_4 was diluted to a demanded wt% with deionized water before reaction. Then, the quantified reactants were mixed in the order of diluted H_2SO_4, H_3BO_3, C and $KMnO_4$ in a 250 mL beaker and stirred at a controlled temperature using a water bath. When the reaction finished, the solid phase was washed with deionized water and dipped in water for 2.0 h until pH value of the waste water reached to 6.0-7.0, then filtrated and dried at 50-60 °C for 5.0 h. The influence of various factors on dilatability of the EG_B were optimized through single-factor tests including the dosages of H_2SO_4 (98 wt%), $KMnO_4$, H_3BO_3 and H_2SO_4 concentration, reaction temperature and time. Feasible conditions of EG_B preparation were finally identified as: mass ratio of C:$KMnO_4$:H_2SO_4(98%):H_3BO_3 was 1.0:0.4:5.0:0.6, the concentrated H_2SO_4 was diluted to 78 wt% before reaction; intercalation reaction was totally maintained for 40 min at 40 °C. Initiation expansion temperature (detected with DHG-9075A oven, temperature precision ±0.1 °C, Shanghai, China) [37] and the maximum EV (detected with SX3-4-13 Muffle furnace, temperature precision ±0.1-0.4% °C, Tientsin, China) of the prepared EG_B are 141 °C and 570 mL g^{-1}, respectively.

Compared with EG_B, the referenced EG with only H_2SO_4 as intercalator was prepared at the mass ratio C:$KMnO_4$:H_2SO_4(98%) of 1.0:0.4:5.0 under the same condition mentioned in the preparation of EG_B. Its initial expansion temperature and EV were detected as 150 °C and 500 mL g^{-1}, respectively.

It's obvious that the addition of H_3BO_3 has significant influence on dilatability, reflected by the increase of EV and adjustment of initial expansion temperature. It is known that H_3BO_3 easily dehydrate even at lower temperature; as a result, water vapor would be produced, which is in favor of the increase of EV. At the same time, the intercalated H_2SO_4 reacts with graphite causing release of CO_2, H_2O and SO_2, [7-9] which leads to the expansion of GICs and the formation of the "worm like" expanded graphite particles.[10] The EG_B should show better flame retardancy than EG for its good dilatability.

Measurements and characterization: EDS of Ca, Mn, S, Si in EG_B and referenced EG was detected with KYKY2800B scanning electron microscope (China) under an accelerating voltage of 20 kV. The detector resolution and the element detection range were 132 eV and from Na to U, respectively. Prior to observation, the surfaces were coated with a conductive material.

The FTIR spectra of the prepared EG_B and EG were recorded between 4000-400 cm^{-1} using a FTIR spectrometer (FTS-40, America Biorad) with a resolution of 2 cm^{-1}.

XRD pattern was obtained with an Y2000 X-ray diffractometer (Dandong, China), under the operation condition of 40 kV, 30 mA, employing Ni-filtered Cu K_α radiation with 2θ ranging from 10° to 70°.

FRs were added into melting LLDPE (processing temperature was not less than 120 °C) in Muller (Jiangsu, China), the mixtures were pressed at 140 °C and 10 MPa, and then chopped into slivers with size of 120.0×6.0×3.0 mm^3 and 127.0×13.0×3.0 mm^3, respectively.

LOI test was used to evaluate the combustion property of the flame retarded LLDPE composites with a size of 120.0×6.0×3.0 mm^3, and it was detected using a JF-3 LOI instrument (Chengde, China) according to Standard of GB/T2406-1993. At the same time, vertical burning tests were performed using a HC-3 vertical burning instrument (Tientsin, China) on sheets of size 127.0×13.0×3.0 mm^3 according to the standard UL 94-1996.

In thermal analysis of TG/DTG (STA 449C, Germany), about 10.0 mg sample, laid in porcelain crucible, was detected under N_2 atmosphere with a flux of 25 mL min^{-1} and heated from about 35 °C to 800 °C at a heating rate of 10 °C min^{-1}. A TM3000 Electron microscope (Japan) was used to observe the surface and section morphology of specimens.

RESULTS AND DISCUSSION

EDS analysis of material and GICs: EDS results listed in Table 1 present the main surface elements except carbon, oxygen and boron (the element detection range of the used detector is from Na to U) and their relative percentage composition in natural graphite, EG_B and referenced EG, respectively. As can be seen, except C element, the natural graphite still consists of S, Mn, Si and Ca. In the referenced EG, the S content is relative higher, which reveals the intercalation of H_2SO_4/HSO_4^-.[10] Although the S content in EG_B is still higher than that of natural graphite, it's lower than that of EG, which dues to the assistant intercalation of H_3BO_3. Therefore, EG_B will release less SO_2 gas than the referenced EG.

Table 1 Surface composition of natural graphite, EG and EG_B determined by EDS [a]

Element relative wt%	Specimens		
	Natural graphite	EG_B	Referenced EG
Si	2.56	5.3	3.8
S	65.2	75.2	83.6
Ca	6.98	7.4	2.8
Mn	20.9	12.1	9.8
Total	95.6	100.0	100.0

[a] The detector resolution and the element detection range were 132 eV and from Na to U, respectively.

FTIR analysis of material and GICs: Figure 1 shows FTIR spectra of the prepared EG_B and referenced EG. As can be seen from the results, two samples both show the characteristic stretching vibrations absorption peaks of -OH (3430-3420 cm^{-1}), caused by intercalation of H_2SO_4/HSO_4^- or H_3BO_3. At the same time, the peaks at about 1620 cm^{-1} are the specific absorption peaks of C=C stretching vibration, originating from graphite conjugated structure. The strong stretching vibration absorption peak of S=O is observed in EG (1118 cm^{-1}), but there are strong superimposed peaks at 1463 cm^{-1} and 1190 cm^{-1} in the FTIR of EG_B, it is because the absorption peaks of S=O and B=O are both appear in the range of 1500-1100 cm^{-1} as reported. [38] Furthermore, the peaks in the range of 800-600 cm^{-1} in the EG_B belong to B-O specific absorption. [39] The results indicate the intercalation of intercalators.

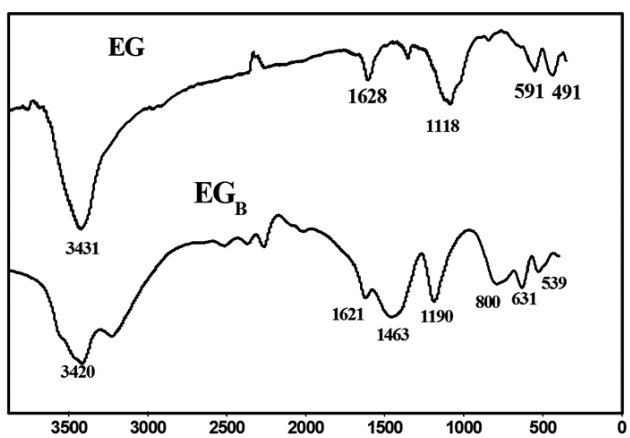

Figure 1 FTIR analysis of the referenced EG and EG_B

Morphology property of natural graphite and EG_B: Figure 2 presents electron microscope photographs of natural graphite and EG_B. As shown in Figure 2 (a) the cross-section of natural graphite (amplified by a factor of 20000), layer structures of natural graphite are compact, and the layers distance is very small and regular. However, the cross-section of EG_B (shown in Figure 2 (b), amplified by a factor of 1000) shows that layers distance has been enlarged, and the boundary layers are loose and damaged. It can be inferred that the intercation forces between the EG_B layers are weaken due to the oxidation of $KMnO_4$ and intercalation of H_2SO_4 and H_3BO_3.

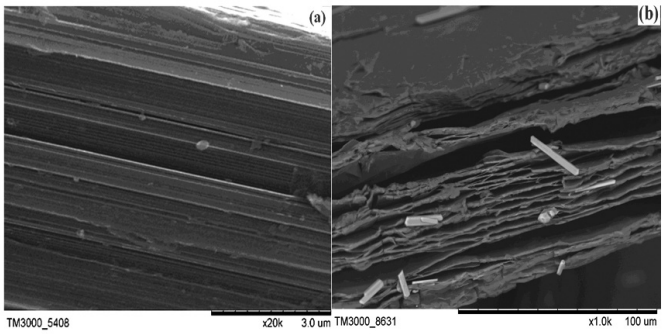

Figure 2 Morphology property of natural graphite (a) and EG_B (b)

XRD analysis of the GICs: XRD analysis for natural graphite, EG_B and the referenced EG were performed. As shown in Figure 3 (a), the two peaks at 26.4° (corresponding an interplanar crystal spacing of 0.334 nm) and 55.5° (corresponding an interplanar crystal spacing of 0.167 nm) are two characteristic peaks of natural graphite. While, XRD patterns in Figure 3 (b) and (c) all show two similar peaks as natural graphite in the range of 25°-27° and 50°-60°, which indicates both EG and EG_B all keep the same layer structure as natural graphite. But it is worthy to note that the diffraction peaks in the range of 25°-27° transfer to smaller angle of 26.3° and 26.2°, respectively. At the same time, each corresponds to a big interplanar crystal spacing of 0.338 nm for EG and 0.339 nm for EG_B. This can be explained that natural graphite is oxidized by $KMnO_4$ and then exhibited positive charge. Then gap between graphite layers is extended due to the repulsion, and intercalating reaction can proceed between graphite and intercalator. The positive charge of the oxidized graphite network is balanced by negatively charged acid anions and also includes acid molecules. [36, 40, 41] Results confirm that intercalators have been inserted into graphite layers.

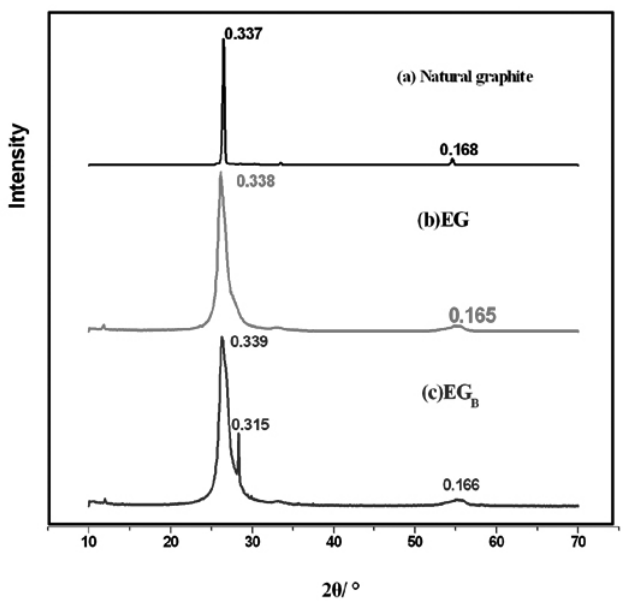

Figure 3 XRD analysis of natural graphite (a), EG (b) and EG_B (c)

Flame Retardancy of composites: The processing temperature of LLDPE is normally lower than 120 °C, so the prepared GICs can be used as FRs. The flame retarded LLDPE specimens were prepared following the above mentioned method, weight percentage between FRs and polymer was listed in Table 2. LOI detection and vertical combustion tests were carried out to evaluate flame retardancy and observe ignition, expansion-extinguishing process, melt-dripping phenomenon. The results were also listed in Table 2.

Table 2 Specimen components and their combustion properties [b]

Specimens	LOI %		UL-94 Level	Melt Dripping
	LOI_{exp}	LOI_{cal}		
100 LLDPE	17.6		-	Yes
70LLDPE/30EG	25.1		V-1	No
70LLDPE/30EG_B	30.2	23.8	V-0	No
70LLDPE/30H_3BO_3	19.2		-	Yes
70LLDPE/18EG/12H_3BO_3	26.5	23.8	V-1	No
70LLDPE/30APP	20.0		-	Yes
70LLDPE/20EG_B/10APP	33.0	26.8	V-0	No
70LLDPE/15EG_B/15APP	32.4	25.1	V-0	No
70LLDPE/10EG_B/20APP	32.0	23.4	V-0	No

[b] Component contents are expressed as wt%. 70LLDPE/18EG/12H_3BO_3 specimen is prepared by mechanical mixing of LLDPE (70 wt%) with the referenced EG (18 wt%) and H_3BO_3 (12 wt%). Furthermore, the ratio of EG:H_3BO_3 (18:12) was calculated according to the ratio of C:H_3BO_3 (determinate to be 1:0.6) in EG_B preparation (herein, it was supposed that all H_3BO_3 were inserted in the intercalation reaction).

As shown in Table 2, LOI of pure LLDPE is only 17.6%, and the combustion accompanies with serious molten drop at the same time (as shown in Figure 4 (a)). LOI values of flame retarded LLDPE composites are all higher than that of pure matrix. Addition of 30 wt% referenced EG improves the LOI of 70LLDPE/30EG composite to 25.1%, and the UL-94 level reaches V-1. Noticeably, the addition of the same amount of the prepared EG_B improves LOI value and UL-94 level of 70LLDPE/30EG_B to 30.2% and V-0 respectively. These results indicate the assistant intercalation of H_3BO_3 obviously improves flame retardancy for LLDPE. This is because the intercalated H_3BO_3 can not only play an retardant role, but also its thermo-decomposition residues B_2O_3 can also increase the cohesiveness and density of the protective intumescent carbonaceous char generating from EG expansion, [42-44] which is helpful to improving its shielding, adiabaticity and protecting the polymeric matrix from degrading into gases. While, the addition of EG_B or EG can all reduce the dripping phenomena and raise the fire safety property, which is attributed to the protective intumescent carbonaceous char (as shown in Figure 4 (b) and (c)) formed on polymer surface by EG_B or EG expansion. It can be seen that the mechanical mixture of H_3BO_3 with LLDPE make 70LLDPE/30H_3BO_3 show a weaker flame retardancy than the referenced EG, but its combination with EG presents an improved anti-flame efficiency, indicating a higher LOI value of 26.5% than the theoretic calculated LOI value of 23.8%. Remarkably, the chemical intercalated H_3BO_3 in EG_B is more effectual than the simple mechanical mix. The most probable reasons should be that the mixing uniformity of H_3BO_3 with graphite is higher in EG_B than the mechanical mix of EG with H_3BO_3. [29, 30]

At the same time, the anti-flame efficiency of APP for LLDPE and its synergetic efficiency with EG_B were investigated. When it is solely added at 30 wt%, LOI of the 70LLDPE/30APP specimen is only improved to 20.0%, and the melt-dripping and ignition still can not be avoided. While, addition of EG_B and APP at different wt% to LLDPE show that the combination can not only increase LOI value, but also all improve the UL-94 level to V-0 simultaneously. Meanwhile, LOI values were all obviously higher than the calculated LOI_{cal} according to the single EG_B wt%, APP wt% and their LOI values. Therefore, it may be inferred that there is synergistic efficiency between the two FRs. Meanwhile, the APP/EG_B ratio has an important influence on flame retardancy, and the tested optimum component is 10:20 as shown in 70LLDPE/10APP/20EG_B specimen, the LOI and UL-94 level are 33.0% and V-0 respectively.

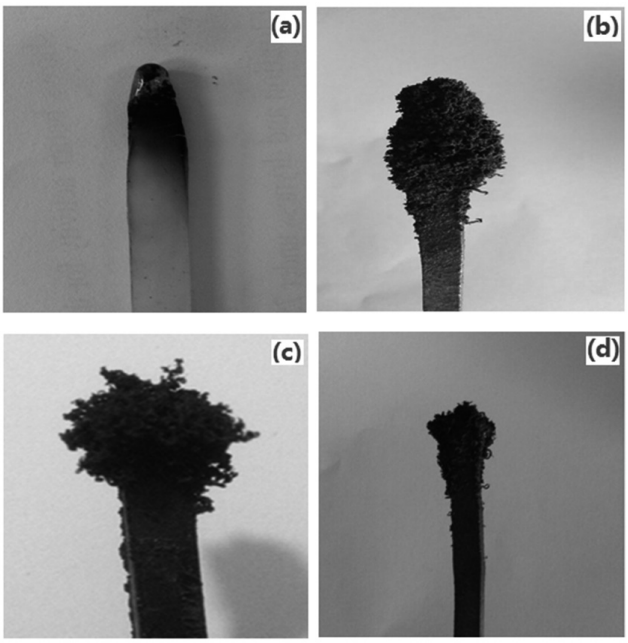

Figure 4 The combustion behavior of LLDPE specimens in vertical burning tests LLDPE (a); 70LLDPE/30EG_B (b); 70LLDPE/30EG (c); 70LLDPE/20EG/10APP (d)

Morphology of the combustion residue: In the burn process, the formation of effective protective char can improve flame retardancy. Therefore, residue morphology of the flame retarded LLDPE after their LOI tests were examined by electron microscope. Figure 5 (a) shows the incision section of 70LLDPE/30EG_B composite after combustion, a regular "open-cellular" structure on the surface is observed due to the expansion of EG_B (showing the "popcorn effect") , originating from blowing gases in redox reaction between residual H_2SO_4 and the graphite. Finally, discontinuity and low mechanical strength of the residue cause the 70LLDPE/30EG_B system easily break and a decrease of shielding function for heat and mass transfer (the tensile strength of 70LLDPE/30EG_B is detected as 6.8 MPa). The residue incision section of 70LLDPE/10APP/20EG_B shown in Figure 5 (b) is relatively continuous and compact due to the conglutination of APP decomposition products (the tensile strength of 70LLDPE/10APP/20EG_B is detected as 7.3 MPa); [17] this structure inhibits the "popcorn effect" and provides a shield that insulates the substrate from radiant heat, and avoids the direct contact between substrate and flame. It is the continuous and compact residual that makes 70LLDPE/10APP/20EG_B composite hold higher LOI value and thermal stability than 70LLDPE/30EG_B composite.

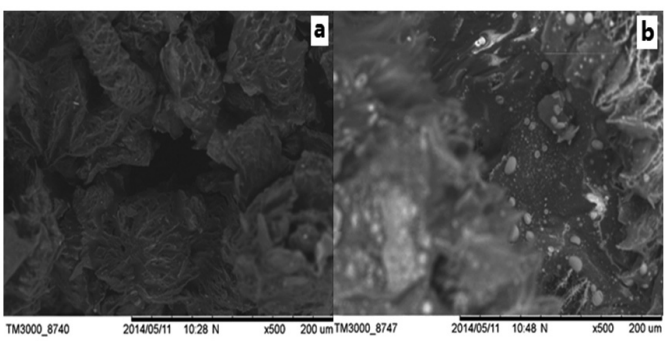

Figure 5 Electron microscopy morphology of 70LLDPE/30EG_B (a) and 70LLDPE/10APP/20EG_B (b) after LOI tests.

Thermal stabilities—TG/DTG analysis: Thermal stability of flame retarded LLDPE is related to the addition of FRs. TG/DTG under N_2 atmosphere was used to evaluate the thermal degradation properties of the referenced EG, EG_B, 70LLDPE/30EG, 70LLDPE/30EG_B and 70LLDPE/10APP/20EG_B, and the results were shown in Figure 6 and Table 3.

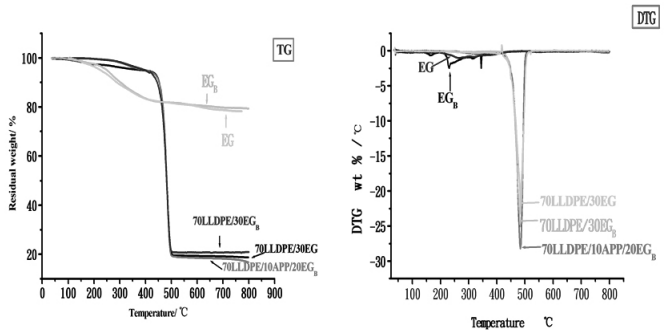

Figure 6 TG and DTG analysis of samples

Table 3 Thermoanalysis data of specimens in N_2 atmosphere [c]

Specimens	$T_{5\%}$	T_{max}	R_{max}	Residue (800 °C)
	/°C	/°C	/(% min^{-1})	/%
EG	248	267	-1.03	78.2
EG_B	223	231	-2.45	79.4
70LLDPE/30EG	396	485	-23.2	18.7
70LLDPE/30EG_B	384	483	-25.0	20.9
70LLDPE/10APP/20EG_B	396	484	-28.2	16.8

[c] T_5 : the temperature at which 5% weight loss occurring, °C.

T_{max}: the temperature corresponding to the maximum decomposition rate, °C.

R_{max}: the maximum decomposition rate, % min^{-1}.

Compared with the flame retarded LLDPE composites, mass loss of the referenced EG and EG_B is more moderate. For EG, the weight lose mainly occurs among 250-450 °C with a peak of 267 °C and the maximum decomposition rate (R_{max}) of -1.03 % min^{-1} as shown in Table 3, wherein CO_2, H_2O and SO_2 gas released during redox reaction between graphite and the intercalated H_2SO_4/HSO_4^-, [16] and leads to the generation of "worm like" expanded graphite. As for EG_B, besides redox reaction between graphite and H_2SO_4, dehydration of the intercalated H_3BO_3 in or between molecules and its fusion occurs in the range of 100-300 °C, which leads to a lower T_5 (temperature at which 5% weight loss occurring), T_{max} (temperature corresponding to the maximum decomposition rate) and higher R_{max} of -2.45 % min^{-1}. Then the produced glassy B_2O_3 coating act as filler and binder for the swollen expanded graphite and then form more compacter carbonaceous char layer as shown in Figure 4 (b). As a result, EG_B keeps a higher residual char yield of 79.4% at 800 °C than the referenced EG of 78.2%, which confirms its higher thermal stability and leads to a relative remarkable flame retardancy indicated by LOI value. [14, 36]

For those flame retarded LLDPE composites with a FR dose of 30 wt% all show the same weight loss tendency, but they hold different T_5, T_{max} and R_{max}. The 70LLDPE/30EG_B composite shows a lower thermal stability than 70LLDPE/30EG composite when the temperature is lower than 490 °C, which is indicated by its lower decomposition temperature corresponding to T_5 and T_{max} and higher R_{max} of -25.0 % min^{-1} as shown in Table 3. The results are caused by the additional decomposition function of the intercalated H_3BO_3 as mentioned in the TG of EG_B. But once the expansion of EG_B, fusion and dehydration of H_3BO_3 finished, the matrix will covered with more residual than 70LLDPE/30EG, which can be indicated by their final residual yield. As for the 70LLDPE/10APP/20EG_B composite, it show a higher R_{max} of -28.2 % min^{-1} than the single EG or EG_B retarded LLDPE. The results are caused by the additional decomposition function of the added APP. As for the residual weight, although 70EVA/10APP/20EG_B system holds a lower residual carbon (caused by the reduced carbon resource) than 70LLDPE/30EG_B system, it presents a higher flame retardancy indicated by LOI. The reason is that with the help of the conglutination of APP decomposing products, the swollen expanded graphite can form a compacter carbonaceous char layer. As for the EG/APP system, the carbonaceous char compaction plays a more important role in improving thermal stability and flame retardancy than the residual carbon weight. [45]

Possible Mechanism of flame retardance: According to the LOI and UL-94 tests results, it can be indicated that the flame retardancy of LLDPE can be greatly improved by EG_B especially the combination of EG_B with APP, which shows a typical synergetic flame retardancy behavior. Through the analysis of TG/DTG and the residual morphology, the synergistic mechanism was proposed for this system. In the gas phase, the non-flammable gases, such as CO_2, SO_2, NH_3, N_2 and H_2O, released through decomposition or dehydration of EG_B, H_3BO_3 and APP, which can dilute the combustible gases. In the condensed phase, EG_B and its intercalated H_3BO_3, the additional added APP play important role in combustion. Initially, the "worm like" char is formed through the expansion of EG_B when the temperature is above 141 °C (initiation expansion temperature of EG_B), but the char is slight [shown as Figure 4 (b)] and can not effectively endure heat flux. Along with the raising of combustion temperature, the further dehydration or fusion of H_3BO_3 occur, and lead to the formation of B_2O_3 glassy coating, which can increase the cohesiveness and density of the protective intumescent char generating from EG_B expansion. At the same time, polyphosphoric acid generated from APP increased the melt viscosity, which can strengthen the char barrier for its strong adhesion effect. The char structure of 70LLDPE/10APP/10EG_B [Figure 4 (d) and Figure 5 (b)] presents a thicker and denser char layer than 70LLDPE/30EG_B [Figure 5 (a)]. Thus, the transfer of gas and heat is retarded by this insulative layer.

CONCLUSIONS

EG_B was successfully prepared with H_2SO_4 and H_3BO_3 as intercalators with chemical oxidation intercalation method. Compared with the referenced EG, the EG_B indicated a better dilatability, flame retardancy and environment-friendly property. EDS, FTIR, SEM and XRD confirmed that the oxidation and intercalation reaction between natural graphite and intercalators could take place. Combustion tests of the flame retarded LLDPE composites showed that EG_B presented a higher LOI value of 30.2% than EG of 25.1%. The combination of EG_B with APP made the 70LLDPE/10APP/20EG_B system showed high efficiency; the LOI value and UL-94 level reached 33.0%, V-0 respectively. TG/DTG analysis proved EG_B and EG_B/APP could improve LLDPE composites thermal stability at high temperature. Electron microscope photographs indicated that the residual char of sample treated with EG_B/APP was more continuous and compact than that of treated with only EG_B. It was concluded that the EG_B/APP system could improve the char quality which was the key factor in dripping resistance and improving thermal stability of the composites.

ACKNOWLEDGEMENTS

The authors would like to thank Natural Science Foundation of Hebei Province (CN) (No. B2015201028) and Seedling Project of College of Chemistry and Environmental Science (Hebei University) for financial support.

REFERENCES

1. J.E. Fischer, T.E. Thompson, *Physics Today* **31**, 36, (2008).
2. G.Q. Liu, M. Yan, *New Carbon Mater.* **17**, 13, (2002).
3. Z.D. Sun, Y.H. Ma, Y. Xu, X.L. Chen, M. Chen, J. Yu, S.C. Hu, Z.B. Zhang, *Polym. Eng. Sci.* **54**, 1162, (2014).
4. C.Q. Wang, F.Y. Ge, J. Sun, Z.S. Cai, *Appl. Polym. Sci.* **130**, 916, (2013).
5. M. Thirumal, D. Khastgir, N.K. Singha, B.S. Manjunath, Y.P. Naik, *Appl. Polym. Sci.* **110**, 2586, (2008).
6. C.F. Kuan, K.C. Tsai, C.H. Chen, H.C. Kuan, T.Y. Liu, C.L. Chiang, *Polym. Composite*. **33**, 872, (2012).
7. H. Shioyama, R. Fujii, Carbon, **25**, 771, (1987).
8. H. Ren, Y.F. Kang, Q.J. Jiao, Q.Z. Cui, New Carbon Mater. **21**, 315, (2006).
9. M.I. Saidaminov, N.V. Maksimova, P.V. Zatonskih, A.D. Komarov, M.A. Lutfullin, N.E. Sorokina, V.V. Avdeev, Carbon, **59**, 337, (2013).
10. S. Duquesne, M.L. Bras, S. Bourbigot, R. Delobel, H. Vezin, G. Camino, B. Eling, C. Lindsay, T. Roels, *Fire Mater.* **27**, 103, (2003).
11. Z.H. Zheng, J.T. Yan, H.M. Sun, Z.Q. Cheng, W.J. Li, H.Y. Wang, X.J. Cui, *Polymer Int.* **63**, 84, (2014).
12. X.L Chen, H. Wu, Z. Luo, B. Yang, S.Y. Guo, J. Yu, *Polym. Eng. Sci.* **47**, 1756, (2007).
13. Z.D. Sun, Y.H. Ma, Y. Xu, X.L. Chen, M. Chen, J. Yu, S.C. Hu, Z.B. Zhang, *Polym. Eng. Sci.* **54**, 1162, (2014).
14. L.L. Ge, H.J. Duan, X.G. Zhang, C. Chen, J.H. Tang, Z.M.J. Li, *Appl. Polym. Sci.* **126**, 1337, (2012).
15. S.G. Hong, S.Y Chang, *Fire Mater.* **36**, 277, (2012).
16. Y.B. Lu, Y.J. Zhang, W.J. Xu, *J. Macromol. Sci.* **50**, 1864, (2011).
17. X.Y. Pang, Y. Tian, M. Q. Weng, Polym. Composite. **36**, 1407, (2015).
18. M.K. Song, *Master's thesis, Hebei Univ.* (2013).
19. S. Duquesne, M.L. Bras, S. Bourbigot, R. Delobel, H. Vezin, G. Camino, B. Eling, C. Lindsay T. Roels, *Fire Mater.* **27**, 103, (2003).
20. L. Chen, Y. Z. Wang, *Polym. Adv. Tech*. **21**, 1, (2010).
21. F.F. Feng, L.J. Qian, *Polym. Composite*. **35**, 301, (2014).
22. Y. Zhang, X.L. Chen, Z.P. Fang, *Appl. Polym. Sci.* **128**, 2424, (2013).
23. H. Seefeldt, U. Braun, M.H. Wagner, *Macromol. Chem. Phys.* **213**, 2370, (2012).
24. L. P. Gao, G.Y. Zheng, Y.H. Zhou, L.H. Hu, G.D. Feng, Y.L. Xie, *Ind. Crop. Prod.* **50**, 638, (2013).
25. L.C. Du, Y.C. Zhang, X.Y Yuan, J.Y. Chen, *Polym-Plast Technol.* **48**, 1002, (2009).
26. D.M. Xu, F. Ding, J. W. Hao, J.X. Du, *Chem. J. Chinese Univ.* **34**, 2674, (2013).
27. O.N. Shornikova, A.V. Dunaev, N.V. Maksimova, V.V. Avdeev, *J. Phys. Chem. Solids*, **67**, 1193, (2006).
28. Y.J. Lee, H.J. Joo, L.R. Radovic, *Carbon*, **41**, 2591, (2003).
29. M.I. Saidaminova, N.V. Maksimovaa, V.V. Avdeeva, *J. Mater. Res.*, **27**, 1054, (2012).
30. M.I. Saidaminov, N.V. Maksimova, N.G. Kuznetsov, N.E. Sorokina, V.V. Avdeev, *Inorg. Mater.*, **48**, 258, (2012).
31. T. Hirata, K.E. Werner, *J. Appl. Polym. Sci.* **33**, 1533, (1987).
32. N. Selvakumar, A. Azhagurajan, T.S. Natarajan, M.M.A. Khadir, *J. Appl. Polym. Sci.* 126, 614, (2012).
33. A.D. Chirico, G. Audisio, F. Provasoli, M. Armanini1, R. Franzese, *Makromol. Chem.* **74**, 343, (1993).
34. S. Ullah, F. Ahmad, P.S.M. Megat Yusoff, *J. Appl. Polym. Sci.* **128**, 2983, (2013).
35. X.M. Hu, D.M. Wang, *J. Appl. Polym. Sci.* **129**, 238, (2013).
36. D.M. Xu, J.W. Hao, G.S. Liu, S.M. Xie, *Acta Polym. Sin*. **7**, 832, (2013).
37. Z.D. Han, D.W. Zhang, L.M. Dong, X.Y. Zhang, *Chinese J. Inorg. Chem.* **23**, 286, (2007).
38. J. Li, S.P. Xia, S.Y. Gao, *Spectrochim. Acta A*, **51**, 519, (1995).
39. C.F. Zuo, *Master thesis, Shanxi Normal University*, (2005).
40. L.B. Ebert, *Annu. Rev. Mater. Sci.* **6**, 181, (1976).
41. H. Zabel, S.A. Solin (Eds). *Springer Series in Materials Science*, **14**, 355, (1990)
42. H. Selig, L.B. Ebert, *Adv. Inorg. Chem. Radiochem.* **23**, 281, (1980).
43. B. Schartel, A. Wei, F. Mohr, M. Kleemeier, A. Hartwig, U. Braun, *J. Appl. Polym. Sci.* **118**, 1134, (2010).
44. C.H. Chen, W.H. Yen, H.C. Kuan, C.F. Kuan, C.L. Chiang, *Polym. Composite.* **31**, 18, (2010).
45. H.F. Zhu, Q.L. Zhu, J. Li, K. Tao, L.X. Xue, Q. Yan, *Polym. Degrad. Stabil.* **96**, 183, (2011).